Editors' Suggestion

Design Principles for High-Temperature Superconductors with a Hydrogen-Based Alloy Backbone at Moderate Pressure

Zihan Zhang,[1] Tian Cui,[2,1,*] Michael J. Hutcheon,[3] Alice M. Shipley,[3] Hao Song,[1] Mingyang Du,[1] Vladimir Z. Kresin,[4] Defang Duan,[1,†] Chris J. Pickard,[5,6] and Yansun Yao[7]

[1]*State Key Laboratory of Superhard Materials, College of Physics, Jilin University, Changchun 130012, China*
[2]*Institute of High Pressure Physics, School of Physical Science and Technology, Ningbo University, Ningbo 315211, China*
[3]*Theory of Condensed Matter Group, Cavendish Laboratory, University of Cambridge, J. J. Thomson Avenue, Cambridge CB3 0HE, United Kingdom*
[4]*Lawrence Berkeley Laboratory, University of California, Berkeley, California 94720, USA*
[5]*Department of Materials Science & Metallurgy, University of Cambridge, 27 Charles Babbage Road, Cambridge CB3 0FS, United Kingdom*
[6]*Advanced Institute for Materials Research, Tohoku University, 2-1-1 Katahira, Aoba, Sendai 980-8577, Japan*
[7]*Department of Physics and Engineering Physics, University of Saskatchewan, Saskatoon, Saskatchewan S7N 5E2, Canada*

(Received 15 May 2021; revised 28 September 2021; accepted 24 December 2021; published 28 January 2022)

Hydrogen-based superconductors provide a route to the long-sought goal of room-temperature superconductivity, but the high pressures required to metallize these materials limit their immediate application. For example, carbonaceous sulfur hydride, the first room-temperature superconductor made in a laboratory, can reach a critical temperature (T_c) of 288 K only at the extreme pressure of 267 GPa. The next recognized challenge is the realization of room-temperature superconductivity at significantly lower pressures. Here, we propose a strategy for the rational design of high-temperature superconductors at low pressures by alloying small-radius elements and hydrogen to form ternary H-based superconductors with alloy backbones. We identify a "fluorite-type" backbone in compositions of the form AXH_8, which exhibit high-temperature superconductivity at moderate pressures compared with other reported hydrogen-based superconductors. The $Fm\bar{3}m$ phase of $LaBeH_8$, with a fluorite-type H-Be alloy backbone, is predicted to be thermodynamically stable above 98 GPa, and dynamically stable down to 20 GPa with a high $T_c \sim 185$ K. This is substantially lower than the synthesis pressure required by the geometrically similar clathrate hydride LaH_{10} (170 GPa). Our approach paves the way for finding high-T_c ternary H-based superconductors at conditions close to ambient pressures.

DOI: 10.1103/PhysRevLett.128.047001

Hydrogen, the lightest element, has been predicted to become a metallic solid exhibiting high-temperature superconductivity (with T_cs in the range 100–760 K) under extreme pressures [1,2]. However, metallization of solid hydrogen is still uncertain in high-pressure experiments up to about 400 GPa [3,4]. It was predicted that comparable high-temperature superconductivity could be achieved in hydrogen dominant materials by "chemically precompressing" the hydrogen with other elements to produce the valence density sufficient for metallization at lower pressures [5]. Based on this principle, a series of H-based superconductors were predicted, and some successfully synthesized in the laboratory. Notably, H_3S was predicted to be a high-temperature superconductor with a T_c of 191–204 K [6], which was later confirmed by an experimentally measured T_c of 203 K at 155 GPa [7,8]. Following this success, several new hydrides in the clathrate hydride family, which consist of a pure hydrogen backbone precompressed by heavy metal atoms, were predicted and then synthesized, including LaH_{10} with a T_c of 250–260 K at 170–180 GPa [9–12]. Several geometric classes of hydrides were found to facilitate high T_c. In addition to the covalent sixfold cubic H_3S and the sodalite-type clathrate hydrides, a class of "pentagraphene-like" hydrides with high T_c were recently predicted at 250 GPa [13]. Although the pressures at which these H-based superconductors become stable (>150 GPa) are much lower than the pressure required to metallize pure hydrogen, they are still difficult to obtain. The next challenge is therefore the realization of room-temperature superconductivity at significantly lower pressures, with a clear final goal of reaching ambient pressure.

Various routes have been explored to reduce the stable pressure of H-based superconductors. Doping known hydrogen-rich binary systems with dopant elements or molecules is one way to achieve this. For example, doping a H_3S host with CH_4 molecules leads to a metastable compound at a much lower pressure of 100 GPa [14,15]. A careful choice of the elements used for precompression is also important. For example, low-pressure stability in lanthanide and actinide

systems correlates strongly with f electrons. As a result, metastable phases of YbH_6 and LuH_6 are predicted to have high-T_c superconductivity at relatively low pressures (145 K at 70 GPa and 273 K at 100 GPa, respectively [16]). Turning to even lower pressures, $Fm\bar{3}m$ $UH_{8+\delta}$ [17], $F\bar{4}3m$ EuH_9 [18], and $C2/c$ NdH_7 [19] have been observed experimentally at 42, 86, and 85 GPa, respectively, but the T_cs in these systems are very low.

While binary hydrides have been extensively explored [20–23], research in ternary hydrides is more challenging, but rewarding. Many ternary hydrides have been found to exhibit favorable properties when compared to current binary systems. For example, C doped H_3S possesses a much higher T_c than that of H_3S in experiments [24], and Li_2MgH_{16}, a molecular Mg-H phase doped with Li, is predicted to have the highest T_c to date (473 K) [25]. However, the phase diagrams of ternary systems are much more complex than those of binary systems and therefore require efficient methods to construct. A recent study shows that a hard-sphere model could help to construct the ternary phase diagram of hydrides at high pressure [26]. The ability to efficiently explore ternary hydrides and identify those with desirable superconducting properties at low pressures is key to advancing research in superconductivity.

Here, we propose a strategy to design high-T_c ternary H-based superconductors at low pressures by engineering binary X—H backbones, which are subsequently "precompressed" by a metal element A. The resulting X—H backbones are easier to metallize than pure H backbones and can be designed by doping known structures with additional atoms (X), which break the local motif of the parent structure. This leads to a metallic H-rich phase with occupied overlapping bands, known as a *hydrogen alloy* phase [5]. We first designed a novel class of fluorite-type ternary structures AXH_8 ($Fm\bar{3}m$), from which we found seven dynamically stable H-based superconductors consisting of a "precompressor" element A (A = Sc, Ca, Y, Sr, La, Ba) and a small-radius element X (X = Be, B, Al). This is followed by the construction of a hard-sphere model to investigate new fluorite-type hydrides and the stability of these new materials in terms of geometrical factors.

We design the first of these alloy backbone materials from the pure H backbone of the high-temperature superconductor LaH_{10} [12], which possesses the same symmetry as the low-pressure UH_8 superconductor [17]. Comparing the crystal structures of UH_8 and LaH_{10} [Figs. 1(a) and 1(b)], the structure of LaH_{10} can be viewed as a UH_8 parent structure doped with additional H atoms at vacant tetrahedral sites. The extra H atoms break the localization of cubic H_8 units and lead to the famous clathrate backbone in LaH_{10}. Instead, dopant X atoms can be inserted in vacancy sites at the center of the cubic H_8 units, resulting in an $Fm\bar{3}m$ structure of $LaXH_8$ [Fig. 1(c)]. For example, Be may be a suitable dopant at these cubic sites. This novel H-Be alloy backbone corresponds to a fluorite-type arrangement [Fig. 1(d)], in

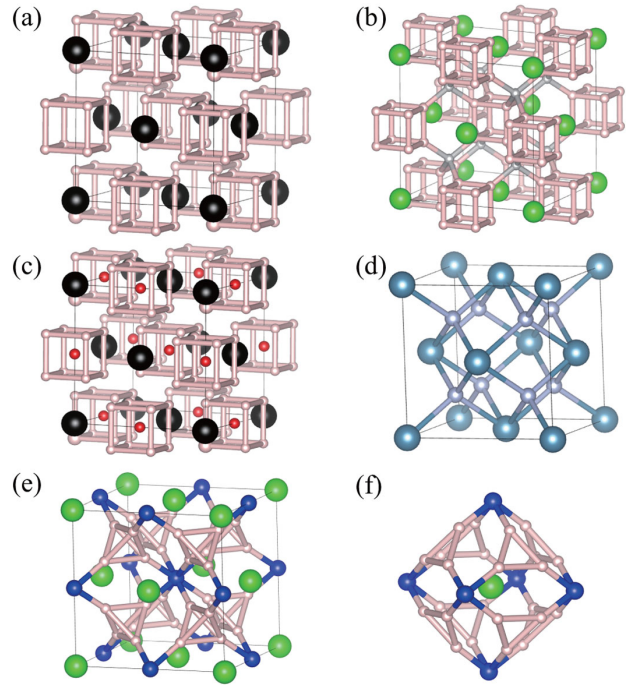

FIG. 1. (a) The crystal structure of UH_8 with $[H_8]$ cubic units. The U ions are shown in black and the H ions in pink. (b) The crystal structure of LaH_{10}, in which La ions are shown in green. The backbone in LaH_{10} consists of cubic-unit H atoms (pink) and tetrahedron-center H atoms (gray). (c) The crystal structure of UH_8, with $[H_8]$ cubic centers shown as red balls. (d) The crystal structure of fluorite CaF_2, the Ca cations are shown in dark blue, and the F ions in light blue. (e) The crystal structure of $LaBeH_8$. The backbone in $LaBeH_8$ consists of tetrahedral-unit H atoms (pink) and cubic-center Be atoms (blue). (f) The fluorite-type cage of $LaBeH_8$.

which Be atoms are located on the sites of a face-centered cubic lattice, and $[H_4]$ tetrahedra are present in the tetrahedral vacancies found between the Be atoms [Figs. 1(e)–1(f)]. Ternary hydrides AXH_8, designed with X—H alloy backbones, potentially achieve high-temperature superconductivity at lower predicted pressures than the required pressures of other reported H-based superconductors.

Having identified this fluorite-type ternary structure, we go on to investigate the wider class of fluorite-type backbone hydrides AXH_8 ($Fm\bar{3}m$), consisting of a precompressor element A (A = Sc, Ca, Y, Sr, La, Ba) and a small-radius element X (X = Be, B, Al). Among the resulting 18 combinations for AXH_8 ternary hydrides, seven exhibit regions of dynamic stability within the range of pressures studied in this work, as established by the absence of imaginary frequencies in phonon dispersions (Figs. S1–S8 of Supplemental Material [27]). These hydrides are $LaBeH_8$, $CaBeH_8$, $YBeH_8$, $CaBH_8$, $SrBH_8$, $LaBH_8$, and $LaAlH_8$. Notably, $LaBeH_8$ remains dynamically stable at pressures as low as 20 GPa. The other 11 hydrides are unstable within the studied pressure range, exhibiting imaginary phonon modes that break crystal

symmetry (Figs. S12–S22 of Supplemental Material [27]). Having identified seven dynamically stable fluorite-type hydrides, we go on to determine their thermodynamic stability using *ab initio* random structure searching [30], by constructing convex hulls (Figs. S24–S30 of Supplemental Material [27]). Combining the phonon dispersion analysis (Fig. S1 of Supplemental Material [27]) with enthalpy difference calculations [Fig. 2(b)], we find that cubic $LaBeH_8$ becomes thermodynamically stable above 98 GPa. However, its dynamical stability (metastability) may be retained as low as 20 Gpa. $YBeH_8$ and $SrBH_8$ become thermodynamically stable at 300 Gpa (Fig. S23 of Supplemental Material [27]). The other four hydrides that exhibit dynamical stability, $CaBeH_8$, $CaBH_8$, $LaBH_8$, and $LaAlH_8$, are not thermodynamically stable within the studied pressure range (≤300 GPa), but are likely to become so at much higher pressures. According to the Inorganic Crystal Structure Database, 20% of synthesized materials are metastable, some of which even have positive formation enthalpies. High-pressure synthesis usually involves high temperatures, and therefore the products are often metastable; synthesized diamond and nitrogen allotropes are good examples. The experimentally discovered superconducting systems Si—H [51] and S—C—H [24] are also found to be metastable in theoretical calculations. Anharmonicity was found to play an important role in some superconducting hydrides [52,53]. However, current calculations do not allow a high-throughput evaluation of anharmonic effects in structure prediction.

Having investigated the stability of these fluorite-type backbone hydrides, we go on to investigate their superconducting properties. From the Eliashberg equations in Sec. 3 of Supplemental Material [27], the values of T_c were determined using $\mu^* = 0.1$. As shown in Fig. 3, $LaBeH_8$ is predicted to exhibit high-temperature superconductivity with a T_c of 192 K at 100 GPa and 183 K at 20 GPa (threshold for metastability). The T_c values calculated using the McMillan equation and Gorkov-Kresin theory are presented and discussed in the Supplemental Material [27]. These fluorite-type backbone structures also have the potential to exhibit room-temperature superconductivity, with the metastable $CaBeH_8$ predicted to possess a T_c of 300 K at 210 GPa. Likewise, we calculate that $YBeH_8$, $CaBH_8$, $SrBH_8$, $LaBH_8$ and $LaAlH_8$ exhibit high-temperature superconductivity within their metastable region, with T_cs of 249 K at 100 GPa, 238 K at 100 GPa, 200 K at 150 GPa, 160 K at 70 GPa, and 144 K at 100 GPa, respectively. A common feature of these superconducting hydrides is the occurrence of soft phonon modes at the Brillouin zone boundary (Figs. S1–S8 in

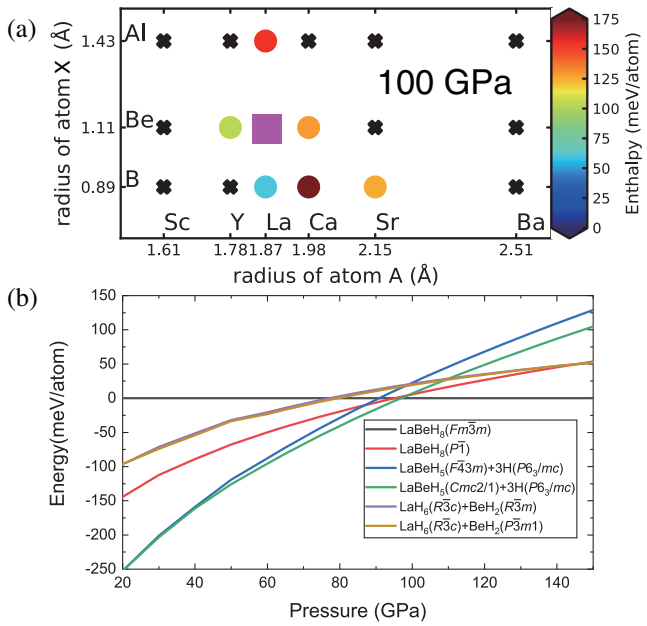

FIG. 2. Calculated enthalpy of fluorite-type hydrides AXH_8. (a) The radius of atom A is plotted on the x axis and the radius of atom X on the y axis. Dynamically unstable systems are shown as black crosses. Metastable phases are shown as circles, colored according to the calculated enthalpy above the convex hull. Thermodynamically stable phases are shown as carmine squares. (b) Calculated enthalpy as a function of pressure for La-Be-H structures relative to the $Fm\bar{3}m$ phase of $LaBeH_8$, where structures of LaH_6, BeH_2, and H are from Refs. [9–11,38,54], respectively.

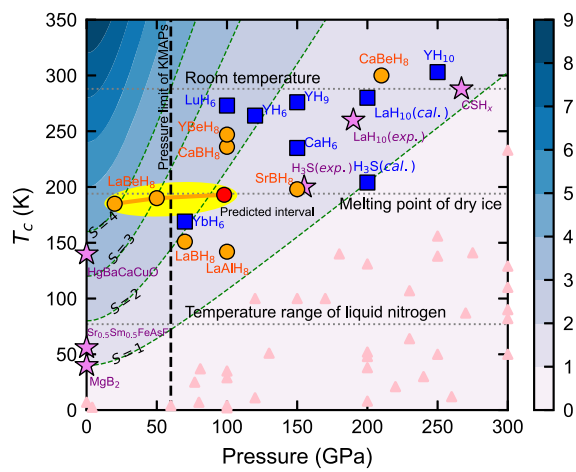

FIG. 3. Pressure dependence of T_cs for typical superconductors. The orange circles are T_cs of fluorite-type backbone hydrides at the lowest pressure where they become dynamically stable. The red circle is at the lowest pressure where $LaBeH_8$ becomes thermodynamically stable (98 GPa), and the suggested synthesis pressure range for cubic $LaBeH_8$ is highlighted in yellow. The blue squares are T_cs of clathrate binary hydrides at the lowest pressures reported in Refs. [6,9,10,39,55]. The purple stars are T_cs of well-known superconductors from experiment [7,12,24,55]. The background is shaded according to the figure of merit $S = (T/\sqrt{P^2 + T^2_{MgB_2}})$ used to evaluate the significance of a particular superconductor [55]. The dotted line is the pressure limit of Kawai-type multianvil presses (KMAPs) [56].

TABLE I. The lattice parameter L, bond lengths $b_{X-\mathrm{H}}$ and $b_{\mathrm{H-H}}$, and flexible factors F calculated from the hard-spheres model (unprimed) and from DFT (primed) at 150 GPa. The amount of charge transferred to H is denoted as δ. Here, we use $t = 1.03$, $d_{\mathrm{H-H}} = 1.1$ Å [9,13,25], $d_{Be-\mathrm{H}} = 1.31$ Å [38], $d_{\mathrm{B-H}} = 1.22$ Å [41], and $d_{\mathrm{Al-H}} = 1.72$ Å [43,60].

	L, Å	$b_{X-\mathrm{H}}$, Å ($F_{X-\mathrm{H}}$)	$b_{\mathrm{H-H}}$, Å ($F_{\mathrm{H-H}}$)	L', Å	$b'_{X-\mathrm{H}}$, Å ($F'_{X-\mathrm{H}}$)	$b'_{\mathrm{H-H}}$, Å ($F'_{\mathrm{H-H}}$)	δ, e-/atom
$LaBeH_8$	5.03	1.25 (91%)	1.52 (137%)	5.17	1.36 (99%)	1.43 (130%)	0.36
$LaBH_8$	5.03	1.25 (102%)	1.52 (137%)	5.13	1.33 (109%)	1.45 (131%)	0.32
$LaAlH_8$	5.03	1.25 (73%)	1.52 (137%)	5.38	1.52 (88%)	1.32 (120%)	0.46
$SrBH_8$	5.79	1.44 (118%)	1.74 (158%)	5.05	1.32 (108%)	1.41 (128%)	0.29
$CaBH_8$	5.33	1.32 (109%)	1.60 (146%)	4.89	1.3 (107%)	1.33 (121%)	0.29
$CaBeH_8$	5.33	1.32 (97%)	1.60 (146%)	4.93	1.32 (96%)	1.32 (120%)	0.32
$YBeH_8$	4.79	1.19 (86%)	1.44 (131%)	5.02	1.34 (98%)	1.36 (124%)	0.40

Supplemental Material [27]), leading to strong electron-phonon coupling. This effect is stronger when the system is close to instability. As shown in Fig. 3, the threshold pressure at which fluorite-type backbone hydrides become dynamically stable is lower than that for typical high-T_c hydrides, while retaining a T_c that is much higher than the temperature of liquid nitrogen. $LaBeH_8$ is the first proposed H-based superconductor with a figure of merit [55] score around $S = 3 - 4$.

Geometrical factors play an important role in the high-throughput screening of materials such as perovskites [57] and MXenes [58]. Effective hard-sphere models can be used as structural prototypes in the exploration of such novel materials [26]. The dynamic stability of fluorite-type hydrides depends on the radii of the precompressor element A, suggesting that a hard-sphere model [59] derived from geometrical factors may allow us to draw general conclusions about this family of structures. To construct this model, we make two simplifications: (i) the "precompressors" A are regarded as hard spheres; (ii) the backbone is characterized by H—H bonds and X—H bonds. The derivation of this model is presented in Sec. 5 of Supplemental Material [27] and the solution gives the lattice parameter of the cubic unit cell (L), the lengths of H—H bonds ($b_{\mathrm{H-H}}$) and X—H bonds ($b_{X-\mathrm{H}}$) as follows:

$$L = \frac{\sqrt{3}+1}{t+1} 2R_A,$$

$$b_{\mathrm{H-H}} = \frac{\sqrt{3}+1-2t}{t+1}\sqrt{6}R_A = F_{\mathrm{H-H}} d_{\mathrm{H-H}},$$

$$b_{X-\mathrm{H}} = \frac{3t-\sqrt{3}}{t+1} R_A = F_{\mathrm{H}-X} d_{\mathrm{H}-X},$$

where R_A is the covalent radius [50] of atom A and $t = 0.95 - 1.05$ is a tolerance factor allowing slight overlap of the hard spheres. The bond lengths can also be represented as products of flexible factors (F) and bond lengths of binary hydrides (d) from the literature.

The solved L, $b_{\mathrm{H-H}}$, and $b_{X-\mathrm{H}}$ for the seven hydrides using the hard sphere model are shown in Table I, alongside the values calculated from DFT at 150 GPa. The value of L obtained in the hard spheres model is similar to that calculated by DFT in the pressure range of 100–200 GPa. The geometry of the fluorite-type backbone has elongated the H—H bond lengths by 30%–60% or 20%–30% (according to the hard-spheres model and DFT, respectively) compared to the H—H bond lengths in common hydrides [9,13,25], because of the large amount of charge transferred to the H—H bond (Table I). The X—H bonds are also affected by the geometry, but whether the bonds are elongated or shortened depends on the composition; with the hard-spheres model and DFT calculations in agreement. Clearly, geometric factors are crucial to understanding the stability of fluorite-type hydrides.

The hard-spheres model captures the general characteristics of AXH_8 and allows us to determine the criteria for elements that can be substituted for X in the crystal. In particular, candidate elements should form bonds to hydrogen with lengths in the range of 1.2–1.6 Å in binary systems. Therefore, we investigate the possibility of substituting Si, P, and S into $LaXH_8$ since the X—H bond lengths are $d_{\mathrm{Si-H}} \sim 1.6$ Å [61], $d_{\mathrm{P-H}} \sim 1.4$ Å [62], and $d_{\mathrm{S-H}} \sim 1.5$ Å [63]. We find that $LaSiH_8$, $LaSH_8$, and $LaPH_8$ are all dynamically stable below 200 GPa (Figs. S9–S11 of Supplemental Material [27]), and they are calculated to exhibit high-T_c superconductivity: 150 K at 100 GPa, 195 K at 200 GPa, and 151 K at 200 GPa (Figs. S50–S52), respectively.

Binary backbones in hydrides typically consist of polar bonds at high pressure. For example, the $[SH_3]$ backbone of SCH_7 consists of H—S polar bonds [see Fig. 4(a)]. End-to-end arrangements of polar bonds in these backbones generally have low enthalpy. But in the $[BeH_8]$ backbone four H atoms with negative charge δ^- are found in close proximity [see Fig. 4(b)], suggesting that the fluorite-type backbone is formed in a different way. In the unique bonding environment of the fluorite-type backbone, a large amount of charge transfer to the H atoms is possible as shown in Table I; these electrons occupy antibonding states along the H—H bonds (Figs. S56–S62 of SM [27]). These extra electrons not only support the elongated H—H bonds,

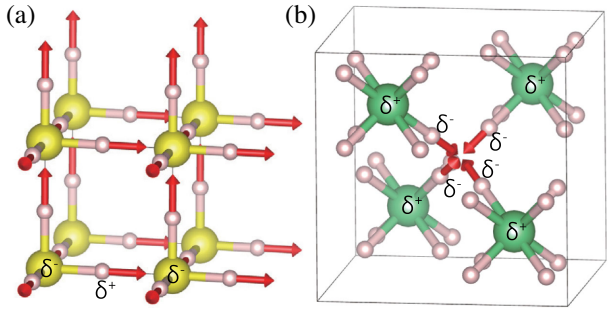

FIG. 4. (a) The polarization vectors of H—S bonds in $[H_3S]$ backbone; in these bonds the positive charge is located at H atoms (pink) and negative charge is located at S atoms (yellow). (b) The polarization vectors of Be—H bonds in $[BeH_8]$ backbone converge, leading to a concentration of charge at the hydrogen atoms. In these bonds the positive charge is located at Be atoms (green) and the negative charge is located at H atoms (pink).

but also give rise to an increased H-derived density of states at the Fermi level. The unique chemistry in alloyed backbones therefore provides a route to improved H-based superconductors.

As part of efforts toward developing H-based superconductors that are stable at low pressure, we design a class of ternary hydrides AXH_8 with fluorite-type alloy backbones. Compared with other reported H-based superconductors, the predicted AXH_8 hydrides exhibit dynamic stability at pressures much lower than their thermodynamic region, while maintaining the strong electron-phonon coupling necessary for high T_c superconductivity. One of the systems we considered, $LaBeH_8$, is dynamically stable down to 20 GPa which is much lower than both the pressure needed to stabilize typical H-based superconductors and the pressure obtainable in KMAPs. The hydrides in the fluorite-type backbone family would have about 20 members if other elements in the lanthanide and actinide series were included. Future investigations of other ternary systems may identify high-temperature superconductors even closer to ambient pressure by similar methods.

In summary, designing hydrides with an alloyed backbone is shown to be an effective approach to obtaining low-pressure H-based superconductors. In these materials, small radius elements are alloyed with hydrogen to introduce new bonds into the backbone structure, replacing some H—H bonds. Our results will stimulate further experimental exploration and the synthesis of hydride-based superconductors at near ambient pressures would represent an important breakthrough in the field of high-temperature superconductivity.

This work was supported by the National Natural Science Foundation of China (Grants No. 12122405, No. 52072188, No. 51632002, No. 11674122), National Key R&D Program of China (Grant No. 2018YFA0305900), Program for Changjiang Scholars and Innovative Research Team in University (Grant No. IRT_15R23), and the Natural Sciences and Engineering Research Council of Canada (NSERC). C. J. P. acknowledges financial support from the Engineering and Physical Sciences Research Council (Grant No. EP/P022596/1) and a Royal Society Wolfson Research Merit award. AMS is funded by an EPSRC studentship. M. J. H. acknowledges the EPSRC Centre for Doctoral Training in Computational Methods for Materials Science for funding under Grant No. EP/L015552/1. Some of the calculations were performed at the High Performance Computing Center of Jilin University and using TianHe-1(A) at the National Supercomputer Center in Tianjin.

Note added.—We note that during the preparation of our manuscript, the same cubic structure was reported in the La-B-H ternary system by two different groups [28,29,64].

*Corresponding author.
cuitian@nbu.edu.cn
†Corresponding author.
duandf@jlu.edu.cn

[1] E. Wigner and H. B. Huntington, On the possibility of a metallic modification of hydrogen, J. Chem. Phys. **3**, 764 (1935).
[2] J. M. McMahon, M. A. Morales, C. Pierleoni, and D. M. Ceperley, The properties of hydrogen and helium under extreme conditions, Rev. Mod. Phys. **84**, 1607 (2012).
[3] P. Dalladay-Simpson, R. T. Howie, and E. Gregoryanz, Evidence for a new phase of dense hydrogen above 325 gigapascals, Nature (London) **529**, 63 (2016).
[4] P. Loubeyre, F. Occelli, and P. Dumas, Synchrotron infrared spectroscopic evidence of the probable transition to metal hydrogen, Nature (London) **577**, 631 (2020).
[5] N. W. Ashcroft, Hydrogen Dominant Metallic Alloys: High Temperature Superconductors? Phys. Rev. Lett. **92**, 187002 (2004).
[6] D. Duan, Y. Liu, F. Tian, D. Li, X. Huang, Z. Zhao, H. Yu, B. Liu, W. Tian, and T. Cui, Pressure-induced metallization of dense $(H_2S)_2H_2$ with high-T_c superconductivity, Sci. Rep. **4**, 6968 (2014).
[7] A. P. Drozdov, M. I. Eremets, I. A. Troyan, V. Ksenofontov, and S. I. Shylin, Conventional superconductivity at 203 kelvin at high pressures in the sulfur hydride system, Nature (London) **525**, 73 (2015).
[8] M. Einaga, M. Sakata, T. Ishikawa, K. Shimizu, M. I. Eremets, A. P. Drozdov, I. A. Troyan, N. Hirao, and Y. Ohishi, Crystal structure of the superconducting phase of sulfur hydride, Nat. Phys. **12**, 835 (2016).
[9] H. Liu, I. I. Naumov, R. Hoffmann, N. W. Ashcroft, and R. J. Hemley, Potential high-T_c superconducting lanthanum and yttrium hydrides at high pressure, Proc. Natl. Acad. Sci. U.S.A. **114**, 6990 (2017).
[10] F. Peng, Y. Sun, C. J. Pickard, R. J. Needs, Q. Wu, and Y. M. Ma, Hydrogen Clathrate Structures in Rare Earth Hydrides at High Pressures: Possible Route to Room-Temperature Superconductivity, Phys. Rev. Lett. **119**, 107001 (2017).

[11] A. M. Shipley, M. J. Hutcheon, M. S. Johnson, R. J. Needs, and C. J. Pickard, Stability and superconductivity of lanthanum and yttrium decahydrides, Phys. Rev. B **101**, 224511 (2020).

[12] A. P. Drozdov, P. P. Kong, V. S. Minkov, S. P. Besedin, M. A. Kuzovnikov, S. Mozaffari, L. Balicas, F. F. Balakirev, D. E. Graf, V. B. Prakapenka, E. Greenberg, D. A. Knyazev, M. Tkacz, and M. I. Eremets, Superconductivity at 250 K in lanthanum hydride under high pressures, Nature (London) **569**, 528 (2019).

[13] H. Xie, Y. Yao, X. Feng, D. Duan, H. Song, Z. Zhang, S. Jiang, S. A. T. Redfern, V. Z. Kresin, C. J. Pickard, and T. Cui, Hydrogen Pentagraphenelike Structure Stabilized by Hafnium: A High-Temperature Conventional Superconductor, Phys. Rev. Lett. **125**, 217001 (2020).

[14] Y. Sun, Y. Tian, B. Jiang, X. Li, H. Li, T. Iitaka, X. Zhong, and Y. Xie, Computational discovery of a dynamically stable cubic SH_3-like high-temperature superconductor at 100 GPa via CH_4 intercalation, Phys. Rev. B **101**, 174102 (2020).

[15] W. Cui, T. Bi, J. Shi, Y. Li, H. Liu, E. Zurek, and R. J. Hemley, Route to high-T_c superconductivity via CH_4-intercalated H_3S hydride perovskites, Phys. Rev. B **101**, 134504 (2020).

[16] Hao Song, Zihan Zhang, Tian Cui, V. Chris J. Pickard, ladimir Z. Kresin, and D. Duan, High T_c superconductivity in heavy rare earth hydrides, Chin. Phys. Lett., **38**, 107401 (2021).

[17] I. A. Kruglov, A. G. Kvashnin, A. F. Goncharov, A. R. Oganov, S. S. Lobanov, N. Holtgrewe, S. Jiang, V. B. Prakapenka, E. Greenberg, and A. V. Yanilkin, Uranium polyhydrides at moderate pressures: Prediction, synthesis, and expected superconductivity, Sci. Adv. **4**, 7 (2018).

[18] D. V. Semenok, D. Zhou, A. G. Kvashnin, X. Huang, M. Galasso, I. A. Kruglov, A. G. Ivanova, A. G. Gavriliuk, W. Chen, N. V. Tkachenko, A. I. Boldyrev, I. Troyan, A. R. Oganov, and T. Cui, Novel strongly correlated europium superhydrides, J. Phys. Chem. Lett. **12**, 32 (2021).

[19] D. Zhou, D. V. Semenok, H. Xie, X. L. Huang, D. F. Duan, A. Aperis, P. M. Oppeneer, M. Galasso, A. I. Kartsev, A. G. Kvashnin, A. R. Oganov, and T. Cui, High-pressure synthesis of magnetic neodymium polyhydrides, J. Am. Chem. Soc. **142**, 2803 (2020).

[20] D. F. Duan, Y. X. Liu, Y. B. Ma, Z. Shao, B. B. Liu, and T. Cui, Structure and superconductivity of hydrides at high pressures, Natl. Sci. Rev. **4**, 121 (2017).

[21] A. R. Oganov, C. J. Pickard, Q. Zhu, and R. J. Needs, Structure prediction drives materials discovery, Nat. Rev. Mater. **4**, 331 (2019).

[22] E. Zurek and T. G. Bi, High-temperature superconductivity in alkaline and rare earth polyhydrides at high pressure: A theoretical perspective, J. Chem. Phys. **150**, 050901 (2019).

[23] J. A. Flores-Livas, L. Boeri, A. Sanna, G. Profeta, R. Arita, and M. Eremets, A perspective on conventional high-temperature superconductors at high pressure: Methods and materials, Phys. Rep. **856**, 1 (2020).

[24] E. Snider, N. Dasenbrock-Gammon, R. McBride, M. Debessai, H. Vindana, K. Vencatasamy, K. V. Lawler, A. Salamat, and R. P. Dias, Room-temperature superconductivity in a carbonaceous sulfur hydride, Nature (London) **586**, 373 (2020).

[25] Y. Sun, J. Lv, Y. Xie, H. Liu, and Y. Ma, Route to a Superconducting Phase above Room Temperature in Electron-Doped Hydride Compounds under High Pressure, Phys. Rev. Lett. **123**, 097001 (2019).

[26] R. Koshoji and T. Ozaki, Densest ternary sphere packings, Phys. Rev. E **104**, 024101 (2021).

[27] See Supplemental Material at http://link.aps.org/supplemental/10.1103/PhysRevLett.128.047001 for computational details, phonon band structure of fluorite-type hydrides, the ternary convex hull of fluorite-type backbone hydrides, equations for calculating T_c and related parameters, the hard-sphere model of fluorite-type backbone hydride, the Crystalline Orbital Hamiltonian Population (COHP) and Integrated Crystalline Orbital Hamiltonian Population (ICOHP) of fluorite-type backbone hydride, electronic structure of fluorite-type backbone hydrides, and structural information. (Includes Refs. [9,28–50]).

[28] S. Di Cataldo, C. Heil, W. von der Linden, and L. Boeri, $LaBH_8$: Towards high-T_c low-pressure superconductivity in ternary superhydrides, Phys. Rev. B **104**, L020511 (2021).

[29] X. Liang, A. Bergara, X. Wei, L. Wang, and Y. Tian, Prediction of high-T_c superconductivity in ternary lanthanum borohydrides, arXiv:2107.02553.

[30] C. J. Pickard and Needs, Ab initio random structure searching, J. Phys. Condens. Matter **23**, 053201 (2011).

[31] M. D. Segall, P. J. D. Lindan, M. J. Probert, C. J. Pickard, P. J. Hasnip, S. J. Clark, and M. C. Payne, First-principles simulation: Ideas, illustrations and the CASTEP code, J. Phys. Condens. Matter **14**, 2717 (2002).

[32] G. Kresse and J. Furthmüller, Efficiency of ab-initio total energy calculations for metals and semiconductors using a plane-wave basis set, Comput. Mater. Sci. **6**, 15 (1996).

[33] J. P. Perdew, K. Burke, and Y. Wang, Generalized gradient approximation for the exchange-correlation hole of a many-electron system, Phys. Rev. B **54**, 16533 (1996).

[34] W. Tang, E. Sanville, and G. Henkelman, A grid-based Bader analysis algorithm without lattice bias, J. Phys. Condens. Matter **21**, 084204 (2009).

[35] V. L. Deringer, A. L. Tchougréeff, and R. Dronskowski, Crystal orbital Hamilton population (COHP) analysis as projected from plane-wave basis sets, J. Phys. Chem. A **115**, 5461 (2011).

[36] P. Giannozzi *et al.*, Quantum ESPRESSO: A modular and open-source software project for quantum simulations of materials, J. Phys. Condens. Matter **21**, 395502 (2009).

[37] G. Kresse and D. Joubert, From ultrasoft pseudopotentials to the projector augmented-wave method, Phys. Rev. B **59**, 1758 (1999).

[38] Z. Wang, Y. Yao, L. Zhu, H. Liu, T. Iitaka, H. Wang, and Y. Ma, Metallization and superconductivity of BeH_2 under high pressure, J. Chem. Phys. **140**, 124707 (2014).

[39] H. Wang, S. T. John, K. Tanaka, T. Iitaka, and Y. Ma, Superconductive sodalite-like clathrate calcium hydride at high pressures, Proc. Natl. Acad. Sci. U.S.A. **109**, 6463 (2012).

[40] Z. Shao, D. Duan, Y. Ma, H. Yu, H. Song, H. Xie, D. Li, F. Tian, B. Liu, and T. Cui, Unique phase diagram and superconductivity of calcium hydrides at high pressures, Inorg. Chem. **58**, 2558 (2019).

[41] C. H. Hu, A. R. Oganov, Q. Zhu, G. R. Qian, G. Frapper, A. O. Lyakhov, and H. Y. Zhou, Pressure-Induced Stabilization and Insulator-Superconductor Transition of BH, Phys. Rev. Lett. **110**, 165504 (2013).

[42] Y. Wang, H. Wang, J. S. Tse, T. Iitaka, and Y. Ma, Structural morphologies of high-pressure polymorphs of strontium hydrides, Phys. Chem. Chem. Phys. **17**, 19379 (2015).

[43] I. Goncharenko, M. I. Eremets, M. Hanfland, J. S. Tse, M. Amboage, Y. Yao, and I. A. Trojan, Pressure-Induced Hydrogen-Dominant Metallic State in Aluminum Hydride, Phys. Rev. Lett. **100**, 045504 (2008).

[44] G. M. Eliashberg, Interactions between electrons and lattice vibrations in a superconductor, JETP **11**, 696 (1960).

[45] L. P. Gor'kov and V. Z. Kresin, Colloquium: High pressure and road to room temperature superconductivity, Rev. Mod. Phys. **90**, 011001 (2018).

[46] V. Z. Kresin, S. G. Ovchinnikov, and S. A. Wolf, *Superconducting State: Mechanisms and Materials* (Oxford University Press, Oxford, 2021).

[47] P. B. Allen and R. C. Dynes, Transition temperature of strong-coupled superconductors reanalyzed, Phys. Rev. B **12**, 905 (1975).

[48] S. Poncé, E. R. Margine, C. Verdi, and F. Giustino, EPW: Electron-phonon coupling, transport and superconducting properties using maximally localized Wannier functions, Comput. Phys. Commun. **209**, 116 (2016).

[49] M. Wierzbowska, S. D. Gironcoli, and P. Giannozzi, Origins of low- and high-pressure discontinuities of T_c in niobium, arXiv:cond-mat/0504077.

[50] R. Heyrovska, Atomic, ionic and Bohr radii linked via the golden ratio for elements of groups 1–8 including lanthanides and actinides, Inter. J. Sci. **2**, 63 (2013).

[51] I. A. T. M. I. Eremets, S. A. Medvedev, J. S. Tse, and Y. Yao, Superconductivity in hydrogen dominant materials silane, Science **319**, 1506 (2008).

[52] I. Errea, M. Calandra, C. J. Pickard, J. R. Nelson, R. J. Needs, Y. W. Li, H. Y. Liu, Y. W. Zhang, Y. M. Ma, and F. Mauri, Quantum hydrogen-bond symmetrization in the superconducting hydrogen sulfide system, Nature (London) **532**, 81 (2016).

[53] I. Errea, F. Belli, L. Monacelli, A. Sanna, T. Koretsune, T. Tadano, R. Bianco, M. Calandra, R. Arita, F. Mauri, and J. A. Flores-Livas, Quantum crystal structure in the 250-kelvin superconducting lanthanum hydride, Nature (London) **578**, 66 (2020).

[54] C. J. Pickard and R. J. Needs, Structure of phase III of solid hydrogen, Nat. Phys. **3**, 473 (2007).

[55] C. J. Pickard, I. Errea, and M. I. Eremets, Superconducting hydrides under pressure, Annu. Rev. Condens. Matter Phys. **11**, 57 (2020).

[56] T. Ishii, Z. D. Liu, and T. Katsura, A breakthrough in pressure generation by a Kawai-type multi-anvil apparatus with tungsten carbide anvils, Engineering **5**, 434 (2019).

[57] S. Lu, Q. Zhou, Y. Ouyang, Y. Guo, Q. Li, and J. Wang, Accelerated discovery of stable lead-free hybrid organic-inorganic perovskites via machine learning, Nat. Commun. **9**, 3405 (2018).

[58] N. C. Frey, J. Wang, G. I. Vega Bellido, B. Anasori, Y. Gogotsi, and V. B. Shenoy, Prediction of synthesis of 2D metal carbides and nitrides (MXenes) and their precursors with positive and unlabeled machine learning, ACS Nano **13**, 3031 (2019).

[59] A. V. Smirnov, S. G. Ponomarev, V. P. Tarasovskii, V. V. Rybal'chenko, A. A. Vasin, and V. V. Belov, Hard-sphere close-packing models: Possible applications for developing promising ceramic and refractory materials, GLASS CERAM+ **75**, 345 (2019).

[60] C. J. Pickard and R. J. Needs, Metallization of aluminum hydride at high pressures: A first-principles study, Phys. Rev. B **76**, 144114 (2007).

[61] C. J. Pickard and R. J. Needs, High-Pressure Phases of Silane, Phys. Rev. Lett. **97**, 045504 (2006).

[62] A. Shamp, T. Terpstra, T. Bi, Z. Falls, P. Avery, and E. Zurek, Decomposition products of phosphine under pressure: PH2 stable and superconducting? J. Am. Chem. Soc. **138**, 1884 (2016).

[63] D. Duan, X. Huang, F. Tian, D. Li, H. Yu, Y. Liu, Y. Ma, B. Liu, and T. Cui, Pressure-induced decomposition of solid hydrogen sulfide, Phys. Rev. B **91**, 180502(R) (2015).

[64] S. Di Cataldo, W. von der Linden, and L. Boeri, La-*X*-H hydrides: Is hot superconductivity possible? arXiv:2106.07266.